An Automated Elastic Image Registration Method For CT And MR Brain Images

Wai Law [†], *Dagan David Feng* [†,‡], *Koon-Pong Wong* [†], *Xiuying Wang* [‡]

[†] Centre for Multimedia Signal Processing
Department of Electronic and Information Engineering
The Hong Kong Polytechnic University, Hung Hom, Kowloon, Hong Kong

[‡] Biomedical and Multimedia Information Technology (BMIT) Group
School of Information Technologies
The University of Sydney, Sydney, NSW 2006, Australia

ABSTRACT

In this paper, an automated approach to register CT and MR brain images based on mutual information and landmark features is described. Images are first rigidly registered by maximization of mutual information. Geometrical feature is then exploited by a differential-geometrical operator. Landmarks are searched in the geometrical feature and registered elastically by thin-plate splines. Experimental results of 2D MR-T1 to CT and MR-T2 to CT registration are presented.

1. INTRODUCTION

Study of anatomy and physiology of internal organs is often aided by different imaging modalities that highlight different aspects of the image organs or structures, and the available information are often fused and evaluated to draw clinical conclusions. Image registration is a transformation process that brings two or more images into the same geometrical alignment such that the complementary information available in different images can be easily and accurately assessed [1]-[3]. It has a wide range of clinical applications, which include multimodality fusion, functional brain mapping, image-guided surgery, characterization of anatomical variation (e.g. changes in shape and size) in abnormal tissue over time, and mapping of anatomical and pathological anatomy to a standardized atlas or a computer model. The fundamental assumption of these applications is that a meaningful spatial correspondence between medical images obtained with different imaging modalities such as computed tomography (CT), magnetic resonance (MR) imaging, and emission tomography (PET and SPECT), etc, can be established by image registration. A number of image registration methods have been developed and they can be broadly classified as being either stereotatic-based, anatomical landmark-based, surface-based, and voxel-based, or a hybrid of these frameworks [1]-[3]. Almost all these methods seek to optimize values of a cost function which defines the similarity measures between the images.

The similarity measures can be the sum of squares of the distances between certain homogeneous features or gray values in the two image sets to be registered. While rigid transformations (rotations and translations) are sufficient in most applications, there are many other applications (e.g. anatomic standardization and intrasubject registration), where nonrigid (or elastic) transformations are required to establish spatial correspondence between images.

In this paper, we present an automated elastic registration approach for CT and MR brain images. The registration process is carried out automatically and both voxel intensities information and geometrical features are used for image matching. The registration approach comprises of three stages: (I) maximization of mutual information, which is not dependent on assumptions about relation between image intensities in different modalities; (II) automatic landmark extraction, which extracts landmarks automatically from the skull region upon segmentation from the processed MR and CT images to form landmark point pairs; (III) thin-plate splines transformation, which elastically registers the target image using the extracted landmark point pairs.

2. MATERIALS AND METHODS

A. Maximization of Mutual Information

Mutual information (MI) is the measure of difference in sum of entropies of the individual images at overlap and the joint entropy of the combined images. It makes no assumption of the relation between image intensities in the two images. Denote $H(A)$, $H(B)$ and $H(A,B)$, respectively, the image entropy for images A and B, and the joint entropy of images A and B, the MI of images A and B, $I(A,B)$, can be related to the entropy of the images as

$$I(A,B) = H(A) + H(B) - H(A,B) \qquad (1)$$

where

$$H = -\sum_i p_i \log p_i \qquad (2)$$

H is the average information supplied by a set of i symbols with probability p_i.

Maximization of mutual information is one of the popular approaches for multimodality medical image registration. It is based on an observation that when two similar images are perfectly aligned, the amount of information that is shared by both images is maximized, whereas the amount of information shared is minimized when out of alignment between the images occurred [4]. In other words, if the images are perfectly overlapped, the joint entropy is minimized and the MI is maximized.

B. Automatic Landmark Extraction

When selecting landmarks from CT and MR head images, representative features that can be distinguished from both modalities are preferred. The skin surface in the MR and CT head images is relatively easy to be identified. However, the skin will easily be deformed between scans and therefore it is not a reliable feature for landmark extraction. Instead of the skin surface, the inner and outer tables of the skull can be used because the skull is a relatively rigid structure of the head.

In CT images, the skull region appears with much higher intensity (a ridge), whereas in MR images it appears with much lower intensity (a trough), in comparison to intensity of its neighborhood. In view of this "ridgeness" property, the skull region can be extracted by a ridge-seeking operator, and the landmarks can then be searched along the skull region. There are a number of differential-geometrical operators that approximate ridges well. In this study, the so-called Lvv operator was used [5]. Define a local gradient based coordinate system spanned by a gradient w and its right-handed normal v as:

$$v = \begin{bmatrix} L_y \\ -L_x \end{bmatrix} \quad \text{and} \quad w = \begin{bmatrix} L_x \\ L_y \end{bmatrix} \quad (3)$$

where L denotes the image intensity function and subscripts represent derivatives along specific directions, the second order derivative of L in the v direction, denoted by L_{vv} can be computed as follows:

$$L_{vv} = \frac{1}{\|v\|^2}(v \cdot \nabla)^2 L \quad (4)$$

where $\nabla = (\partial/\partial x, \partial/\partial y)$. Since the Lvv operation uses a gradient-based local coordinate system instead of the usual Cartesian coordinate system, it is invariant under rotations and translations of the object and therefore it appears as a good ridgeness measure.

The skull can be segmented from the head in the ridge image by averaging pixel intensity along the skull region. The inner and outer tables of the skull can be extracted from the identified skull region. Edge detection is performed on the skull tables when they are delineated

from the skull. In a few cases, some of the irrelevant segments may also be delineated simultaneously from the skull and the skull tables, and these segments will introduce weak edges on the edge image, causing erroneous results of landmark localization. To overcome this problem, the edge image needs to undergo a connected component labeling process at which the image is scanned and pixels are grouped into components based on pixel connectivity to form a closed skull region whose centroid is then determined. A circle centered at the centroid is constructed to inscribe the skull region and is divided into $N/2$ sectors, and N landmarks are located at the intersections of the radii of the circle and the boundary of the skull. Note that the angles subtended by the sectors are not necessarily equal. Thus, more landmark points can be extracted along skull boundary with subtle changes. The landmark points are labeled and paired with another set of landmarks obtained in the same fashion from the image acquired by another modality to form landmark point pairs.

C. Thin-Plate Splines

When the landmark point pairs are identified from the landmark extraction, the displacements necessary to map the location of the landmarks in the target (MR) image to the landmarks in the reference (CT) image can be approximated by analytical functions such as high-degree polynomials and splines. Spline is referred to the use of a long flexible strip of wood or metal to model the surfaces of deformed objects. In this study, thin-plate splines were used to model the deformation represented by the extracted landmark points. Thin-plate splines (TPS) [6] are member of a family of splines that are based on radial basis functions. The radial basis function in 2D is defined as:

$$U(r) = r^2 \log(r^2) \quad (6)$$

where $r = \sqrt{x^2 + y^2}$ is the Euclidean distance; U is the fundamental solution of the biharmonic equation $\Delta^2 U = 0$ that satisfies the condition of minimal bending energy [6]:

$$\Delta^2 U = \left(\frac{\partial^2}{\partial x^2} + \frac{\partial^2}{\partial y^2}\right)^2 U = 0 \quad (7)$$

For a TPS function $f(x,y)$, the bending energy of the thin-plate spline function is given by:

$$\iint_{R^2} \left(\left(\frac{\partial^2 f}{\partial x^2}\right)^2 + 2\left(\frac{\partial^2 f}{\partial x \partial y}\right)^2 + \left(\frac{\partial^2 f}{\partial y^2}\right)^2\right) dxdy \quad (8)$$

The TPS model transforms the coordinate of the original image (x,y) into the new coordinate (x',y') by a mapping:

$$(x', y') \mapsto (f_x(x, y), f_y(x, y)) \qquad (9)$$

where $f_x(x,y)$ and $f_y(x,y)$ are the functions of displacements in x- and y-direction, respectively. A TPS interpolation function can be written as:

$$f(x, y) = a_1 + a_x x + a_y y + \sum_{i=1}^{n} w_i U\left(\left|P_i - (x, y)\right|\right) \qquad (10)$$

where the coefficients a define the affine part of the transformation, whereas the coefficients w define the elastic deformation; U is the radial basis function and P_i is the ith landmark point. The advantage of writing the displacement function in this form is that it can be expressed in matrix form as follows:

$$f(x,y) = \begin{bmatrix} a_1 & a_x & a_y \end{bmatrix} \begin{bmatrix} 1 \\ x \\ y \end{bmatrix} + \begin{bmatrix} w_1 & w_2 & \dots & w_n \end{bmatrix} \begin{bmatrix} U(r_1) \\ \vdots \\ U(r_2) \end{bmatrix} \qquad (11)$$

By collecting the affine transformation and the elastic transformation from the sets of landmark point, the coefficients a and w can be solved by matrix inversion [6].

3. EXPERIMENTS

Experiments were carried out to assess the performance of the proposed automated algorithm by registering some deformed MR images to CT images. We presented the results of two experiments: (1) MR-T1 to CT, and (2) MR-T2 to CT image registration. In the first experiment, the MR-T1 image was rigidly registered to CT image in Stage I. The landmark point pairs were then extracted in Stage II. Finally, the MR-T1 image was elastically registered with the CT image in Stage III. The same approaches were used in the second experiment for MR-T2 to CT image registration. The maximization process is accomplished by Powell's method of optimization [7]. Once the maximum value of the mutual information is found, the images should have geometrically aligned.

With the exception of Powell's optimization algorithm that was implemented in C++, all methods were implemented in MATLAB® under Microsoft® Windows® environment. The maximization of MI (Stage I) takes about 10 mins and the total time required to complete all stages is approximately 15 mins on a PC equipped with PIII-866 MHz CPU and 256 MB of memory.

4. RESULTS AND DISCUSSION

Tables 1 and 2 show, respectively, the sequence of images generated from the registration process of MR-T1 to CT and MR-T2 to CT. As expected, the maximization of MI yields good results in correcting the translation and rotation difference between images for a coarse registration. The automatic landmark extraction process can extract landmarks from images with a clear and connected skull region. However, it may fail for brain slices acquired at the top portion of the head. This is because the outer table and the inner table of the skull are connected in these images and it is very difficult to distinguish them by the automatic algorithm without constraints. The identification process of the skull table is generally easier in CT and MR-T2 than that in MR-T1. This may be due to the fact that CT head images have a larger contrast between the skull and the tissues, whereas the MR-T2 head images have a larger contrast between the skull and the CSF. While the skull region appears dark in MR-T1 images, the surrounding tissue appears rather dim as well. Therefore, incorrect landmark extraction may occur more frequently in MR-T1 images.

For the TPS transformation process, deformation near the landmarks was corrected. The registration result was enhanced as the number of landmark points was increased and the landmarks were distributed around deformed regions. When incorporating the landmarks point pairs generated from the automatic landmarks extraction process, images with deformation near the skull can be successfully registered. However, the results were not satisfactory for images with deformation in the inner brain and the scalps, as the landmarks for this region are difficult to be defined.

5. CONCLUSIONS

This paper presents a new MR and CT brain images registration approach based on image intensity information and landmark feature extraction. The target image is first rigidly registered by maximization of mutual information, and then elastically registered by thin-plate splines transformation with landmarks that are extracted automatically with a ridge seeking operator from the skull table. The whole registration process can be carried out automatically, and it is able to register deformed images. The registration yields a good result in correcting the difference in spatial alignment between MR and CT images when deformation occurs. Further research is underway to improve the registration algorithm, especially the automatic landmark extraction process and so as to enhance the accuracy and the robustness of the proposed approach for clinical uses.

6. ACKNOWLEDGEMENT

7. REFERENCES

[1] J.V. Hajnal, D.L.G. Hill, D.J. Hawkes, *Medical Image Registration*, CRC Press, 2001.

[2] P.A. van den Elsen, E.J.D. Pol, and M.A. Viergever, "Medical image matching – a review with classification," *IEEE Eng. Med. Biol. Mag.*, vol. 12, pp. 26-39, 1993.

[3] J.B.A. Maintz and M.A. Viergever, "A survey of medical image registration," *Med. Image Analy.*, vol. 2, pp. 1-36, 1998.

[4] F. Maes, A. Collignon, D. Vandermeulen, G. Marchal, and P. Suetens, "Multimodality image registration by maximization of mutual information," *IEEE Trans. Med. Imag.*, vol. 16, pp. 187-198, 1997.

[5] J.B.A. Maintz, P.A. van den Elsen, and M.A. Viergever, "Extraction of invariant ridge-like features for CT and MR brain image matching," *Proc. Int. Conf. on Volume Image Processing* (M.A. Viergever, ed.), SCVR, Utrecht, pp. 129-132, 1993.

[6] F.L. Bookstein, "Principal warps: thin-plate spline and the decomposition of deformations," *IEEE Trans. Patt. Anal. Machine Intell.*, vol. 11, pp. 567-585, 1989.

[7] W.H. Press, S.A. Teukolsky, W.T. Vetterling, and B.P. Flannery, *Numerical Recipes in C*, 2nd ed., Cambridge University Press, NY, 1992.
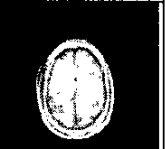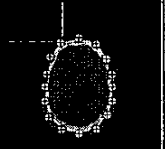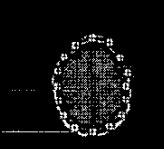
Stage	Combined image before registration	MR-T1 image after registration	Combined image after registration
I			
II	Contour on CT	Contour on MR-T1	Landmarks on CT
II			
III	Landmarks on MR-T1	MR-T1 image after TPS	Combined image after TPS
III			

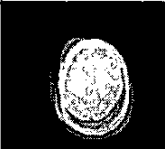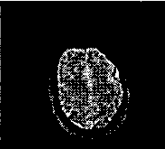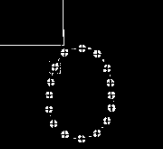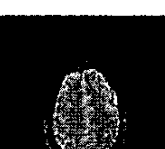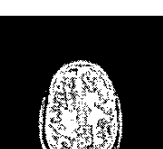Table 1: Sequence of images generated in each stage for the MR(T1) to CT registration.

Stage	Combined image before registration	MR-T2 image after registration	Combined image after registration
I			
II	Contour on CT	Contour on MR-T2	Landmarks on CT
II			
III	Landmarks on MR-T2	MR-T2 image after TPS	Combined image after TPS
III			

Table 2: Sequence of images generated in each stage for the MR(T2) to CT registration.